Dalton Transactions

ROYAL SOCIETY OF CHEMISTRY

COMMUNICATION

View Article Online
View Journal | View Issue

Cite this: *Dalton Trans.*, 2025, **54**, 8035

Received 26th February 2025,
Accepted 27th February 2025

DOI: 10.1039/d5dt00480b

rsc.li/dalton

Isolation of the parent triplet titanocene *via* NHC stabilisation†

Felix Meyer,[a] Serhiy Demeshko,[a] Christopher Golz,[b] Oliver P. E. Townrow *[c] and Malte Fischer *[a]

We present the synthesis and characterization of the parent isolable monomeric triplet titanocene complex, stabilized by the N-heterocyclic carbene (NHC) IMe_4. Investigated by SQUID magnetometry and quantum-chemical calculations, reactivity studies of the titanium precursor $[Cp_2Ti(btmsa)]$ (2) with the NHC $I^iPr_2Me_2$ and the zirconocene complex $[Cp_2Zr(py)(btmsa)]$ (1) revealed divergent reactivity patterns, highlighting the role of steric and electronic effects in stabilization.

Although the Group 4 elements titanium, zirconium, and hafnium show a strong thermodynamic preference for the +IV oxidation state, their complexes in the +II state are becoming increasingly significant in synthetic applications, ranging from catalysis to materials development.[1] Combining Lewis acid reactivity in the +IV state and reductive transformations in the +II state, systems capable of reversible redox cycling between these have the potential to unlock exciting new possibilities for utilizing these Earth-abundant elements in efficient redox catalysis.[1,2] Additionally, paramagnetic titanium(III) organometallics have also found recent attention as molecular spintronic components based on Earth-abundant metals, adding further relevance to finding novel examples.[3]

However, due to the thermodynamic stability of the +IV oxidation state, accessing low-valent species typically requires 'masking' through the incorporation of redox non-innocent ligands or ligands with pronounced backbonding capabilities (*e.g.* alkenes and alkynes). These ligands provide access to controlled sources of the low-valent form, serving as synthons for its generation.[1,2,4] A key factor in advancing this field is a deep understanding of the electronic structure and nature of truly isolable low-valent Group 4 compounds and intermediates. Unlike their later transition metal homologues, titanocene and zirconocene $[Cp_2M]$ (Cp = η^5-cyclopentadienyl; M = Ti, Zr) are not isolable and decompose through C–H activation processes.[5] It must be noted that even the permethylated derivative $[Cp^*_2Ti]$ (Cp^* = η^5-pentamethylcyclopentadienyl) is unstable and, for example, readily coordinates dinitrogen.[6] However, its magnetic moment could be determined and was found to be in between 2.48 (129 K) and 2.60μ_B (298 K), slightly lower than the spin-only value of 2.83μ_B, and consistent with the presence of two unpaired electrons.[6] Through the incorporation of bulky silyl groups at the cyclopentadienyl ligands, several triplet titanocene derivatives have been isolated and structurally characterized, such as $[\{C_5Me_4(SiMe_2{}^tBu)\}_2Ti]$, which has a magnetic moment of 2.40 μ_B.[7] The reactive parent Group 4 metallocene fragment $[Cp_2M]$ is typically generated *in situ* by use of soluble, closed-shell-singlet synthons through the release of CO, PMe_3, alkenes, alkynes, or by mixing $[Cp_2MCl_2]$ with strong reducing agents.[1c,4,8,9] Notable examples include ($[Cp_2ZrCl_2]$/^{n}BuLi),[10] $[Cp_2Ti(PMe_3)_2]$,[11] $[Cp_2Ti(CO)_2]$ (Scheme 1),[12] and btmsa (bis(trimethylsilyl)acetylene) complexes $[Cp_2Zr(py)(btmsa)]$ (**1**) (py = pyridine), and $[Cp_2Ti(btmsa)]$ (**2**).[1c,4,8,13] Their chemistry

[a]*Institut für Anorganische Chemie, Georg-August-Universität Göttingen, Tammannstraße 4, D-37077 Göttingen, Germany.*
E-mail: malte.fischer@uni-goettingen.de
[b]*Institut für Organische und Biomolekulare Chemie, Georg-August-Universität Göttingen, Tammannstraße 2, D-37077 Göttingen, Germany*
[c]*Institute of Nanotechnology, Karlsruher Institut für Technologie, Hermann-von-Helmholtz-Platz 1, D-76344 Eggenstein-Leopoldshafen, Germany.*
E-mail: oliver.townrow@kit.edu

†Electronic supplementary information (ESI) available: Experimental procedures, characterization of the reported compounds, crystallographic and computational details. CCDC 2419251–2419254. For ESI and crystallographic data in CIF or other electronic format see DOI: https://doi.org/10.1039/d5dt00480b

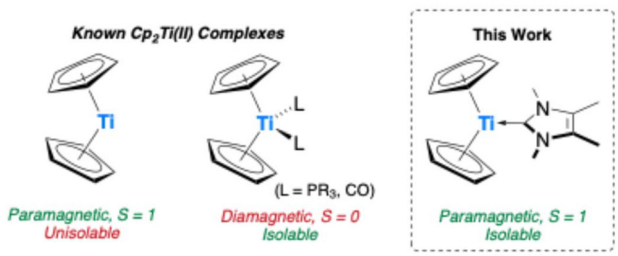

Scheme 1 Examples of bis(cyclopentadienyl)titanium(II) complexes.

has been extensively reviewed on many occasions.[1c,4,8,14] In contrast to these commonly employed diamagnetic Group 4 metallocenes, we present the synthesis and isolation of a crystalline *paramagnetic* parent titanocene, stabilised by an NHC which better mimics the electronic state of free [Cp_2Ti].[5] We further demonstrate how the choice of the metal precursor and NHC is crucial to metallocene formation, as varying these caused either ligand exchange, imidazole tautomerisation, or C–H activation. The reaction of **1** with IMe_4 (1,3,4,5-tetramethylimidazol-2-ylidene) in C_6D_6 at room temperature resulted in an expected clean ligand exchange reaction in which the NHC replaces pyridine to yield [$Cp_2Zr(IMe_4)$(btmsa)] (**3**) (Scheme 2). The ligand exchange is visibly evident by an immediate colour change of the reaction mixture from intense purple to yellow–brown upon NHC addition. Inspection of the ^{1}H NMR spectrum revealed the chemical shifts of free pyridine, in addition to divergence of the Me_3Si signals of the btmsa ligand, indicating that free rotation is now sterically prohibited (Fig. S2†). The ^{13}C chemical shift of the NHC carbene centre is located at $\delta^{13}C\{^1H\}$ = 197.8 ppm, confirmed by ^{1}H/^{13}C HMBC NMR (Fig. S4†), shifted when compared to that of the free carbene ($\delta^{13}C\{^1H\}$ = 213.3 ppm).[15] It is worth noting that neither the addition of a second equivalent of IMe_4 to **3** nor the direct addition of two equivalents of IMe_4 to **1** led to any exchange of btmsa for IMe_4, even at elevated temperatures (Fig. S5†). Yellow crystals of **3** suitable for single-crystal X-ray diffraction (SCXRD) were obtained from a saturated *n*-hexane solution at −30 °C, which allowed for structural confirmation. The coordination environment at zirconium is best described as distorted square pyramidal according to the τ_5 structural parameter (τ_5 = 0.11) (Fig. S6†).[16] The C_{NHC}–Zr bond length of 2.466(3) Å is in good agreement to other IMe_4 ligated zirconium complexes, *e.g.* [(η^7-C_7H_7)(η^5-C_5H_5)Zr(IMe_4)] (2.4452(17) Å).[17,18] Interestingly, no reaction readily occurs between **1** and the slightly larger NHC $I^iPr_2Me_2$ (1,3-diisopropyl-4,5-dimethylimidazol-2-ylidene). However, upon prolonged heating of this mixture up to 90 °C, **1** and $I^iPr_2Me_2$ are completely consumed, and the characteristic signals of free pyridine are observed by ^{1}H NMR spectroscopy. In addition, three signals in the typical range of cyclopentadienyl ligands and two new signals typical of hydride species are found, indicative of the formation of multiple products (Fig. S7†). After several attempts, a few dark yellow crystals were obtained from a saturated *n*-hexane solution at −30 °C, and the structure of the κ^1-imidazole complex **4** was confirmed by SCXRD (Fig. S8†), with structural parameters in good agreement to those of **3**.[19] The formation of **4** suggests that propene is formed as a by-product. However, the expected ABX coupling pattern in the ^{1}H NMR spectrum could not be unambiguously assigned due to the formation of additional byproducts and overlapping signals. Therefore, the headspace of the reaction, performed in toluene as the solvent, was analysed *via* GC-MS, confirming the presence of propene (Fig. S19 and S20†). Furthermore, trimethylsilane, ethyltrimethylsilane, vinyltrimethylsilane, pyridine and the employed solvents were detected, with the presence of the various silanes underscoring the complexity of the reaction's outcome.[19] It is worth noting that although the NHC-to-imidazole transformation is unusual, the reverse imidazole to NHC reactivity pattern has precedence in the literature.[20] We then explored the reactions of these NHCs with the lighter, titanium, analogue [Cp_2Ti(btmsa)] (**2**). Contrary to the formation of **4**, the reaction of **2** with one equivalent of $I^iPr_2Me_2$ in aromatic solvents occurs at room temperature, resulting in the immediate release of btmsa, as confirmed by its ^{1}H NMR chemical shift at 0.16 ppm (Fig. S9†). Although the reaction onset occurred rapidly, full conversion of **2** proceeds slowly and plateaus at around 50% after 72 hours. Heating the mixture to 90 °C for an extended period eventually drives the reaction toward near completion; however, approximately half an equivalent of the NHC remains unreacted, and signs of a paramagnetic product begin to emerge.[19] Upon work-up at this stage, dark violet crystals suitable for SCXRD are consistently obtained, revealing the formation of the hydride-bridged dititanium complex **5** (Fig. 1). Additionally, formal loss of dihydrogen and C–H activation of one cyclopentadienyl ligand led to the formation of bridging fulvalene and cyclopentadienyl

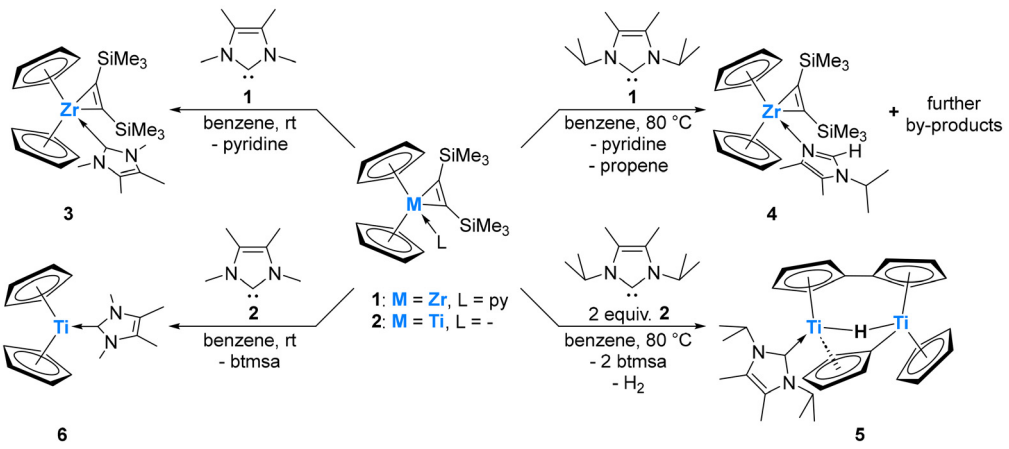

Scheme 2 Reactions of [Cp_2Ti(btmsa)] (**1**) and [Cp_2Zr(py)(btmsa)] (**2**) towards IMe_4 and $I^iPr_2Me_2$ to give complexes **3**, **4**, **5**, and **6**.

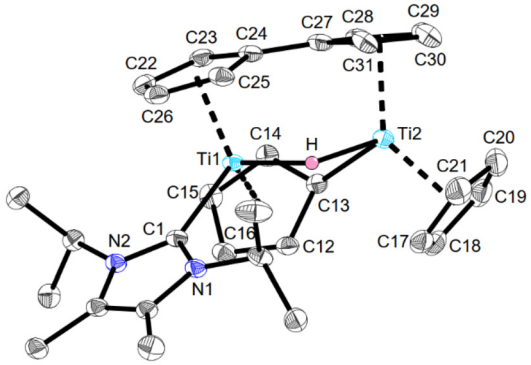

Fig. 1 Molecular structure of **5** in the crystal. Anisotropic displacement parameters are drawn at the 50% probability level, with data collected at 100 K (hydrogen atoms attached to carbon omitted for clarity). Selected bond lengths (Å) and angles (deg): Ti1···Ti2 3.1183(6), Ti1–C1 2.318(2), Ti1–H1 1.92(4), Ti2–C13 2.166(2), Ti2–H1 1.84(4), Ti1–H1–Ti2 112.6, Ct1–Ti1–Ct2 136.0, Ct3–Ti2–Ct4 133.5 (Ct1 = C12–C15, Ct2 = C22–C26, Ct3 = C17–C20, Ct4 = C27–C31).

ligands to both titanium atoms and only one NHC ligation, which explains why approximately half an equivalent of the NHC remains unreacted. The Ti1–C1 bond length is 2.318(2) Å and clearly exceeds the respective single bond covalent radii of the respective elements (Σ_{cov}(Ti–C) = 2.11 Å),[21] indicating expected donor–acceptor interactions. This bond length aligns well with other NHC-ligated titanium hydrides, such as [$(C_8H_4(1,4\text{-}Si^iPr_3)_2)_2${(IMe$_4$)Ti(μ-H)TiH}] (**I**) reported by Tsoureas *et al.*, in which also only one of the titanium(III) centres is coordinated by an NHC (2.300(2) Å).[22] The Ti–H bond lengths (Ti1–H1 1.92(4) Å; Ti2–H1 1.84(4) Å) also compare favourably to **I**, as well as to [(η^5-C_5H_3-1,2-Me_2)$_2$Ti(μ-H)Ti(η^5-C_5H_3-1,2-Me_2)(η^5,η^1-C_5H_2-1,2-Me_2)] (**II**) (1.79(2) Å and 1.91(2) Å).[22,23] Both titanium atoms exhibit a distorted tetrahedral coordination environment according to the τ_4 and τ_4' structural parameters (Ti1: 0.83, 0.73; Ti2: 0.79, 0.73).[24] The Ti2–C13 bond length of 2.166(2) Å is typical of a single bond, falling between the single-bond covalent radii of titanium and carbon (*vide supra*) and matching the analogous bond length in **II** (2.204(2) Å).[21,23] The folding of the fulvalene ligand is evident from a dihedral angle of 17.6(2)° between the two planes defined by both five-membered rings, as well as the inter-ring carbon–carbon bond length of 1.452(4) Å, both of which are diagnostic of fulvalene dititanium complexes (*cf.* [{Cp$_2$Ti(μ-F)}$_2$(μ-η^5:η^5-$C_{10}H_8$)] (1.464(8) Å and 15.3(3)°)).[25] Inspection of the ^{1}H NMR spectrum from crystalline **5** in C_6D_6 at room temperature revealed several broad signals between δ^1H = −25 and +35 ppm, indicative of a paramagnetic compound (Fig. S14†).

Finally, we turned our attention to the remaining combination: [Cp$_2$Ti(btmsa)] (**2**) and IMe$_4$. Upon adding one equivalent of IMe$_4$ to a C_6D_6 solution of **2**, three new broad signals at −29.48, 9.92, and 93.46 ppm were detected alongside the characteristic signal of free btmsa in the ^{1}H NMR spectrum, indicating a rapid ligand exchange reaction that occurs within a few minutes, yielding [Cp$_2$Ti(IMe$_4$)] (**6**) (Scheme 2 and Fig. S16, S17). Slow diffusion of *n*-pentane into a benzene solution of **6** produced dark yellow crystals, allowing for the unambiguous elucidation of the molecular structure by SCXRD (Fig. 2, top). Notably, complex **6** crystallises as dark yellow plates in the triclinic space group $P\bar{1}$, with three independent molecules in the unit cell, mainly due to different orientations of the Cp ligands (eclipsed and staggered conformers observed); the other structural parameters of all three molecules are in very good agreement. The average titanium–C_{NHC} bond length is 2.27 Å, which is slightly shorter compared to the herein reported complex **5**. In relation to a related formal three-coordinate and NHC-ligated titanium complex, such as [(C_6H_6)$_2$Ti(IMe$_2$H$_2$)] (2.323(3) Å), this bond length is reduced and corresponds to the different titanium oxidation states in the two complexes.[26] The titanium centre is in a trigonal planar coordination environment with a pronounced widening of the Ct1–Ti1–Ct2 angle (144.5°). The IMe$_4$ ligand is aligned almost perpendicular to the Ct1–Ti1–Ct2 axis, exhibiting a dihedral angle of 81.8°. The UV-vis spectrum of Cp$_2$Ti(IMe$_4$) reveals an absorption maximum at 389 nm (c = 1 g L^{-1}), in accordance to its (dark) yellow colour (Fig. S18†).

To gain further insight into the electronic ground state of complex **6**, it was investigated using SQUID magnetometry (see

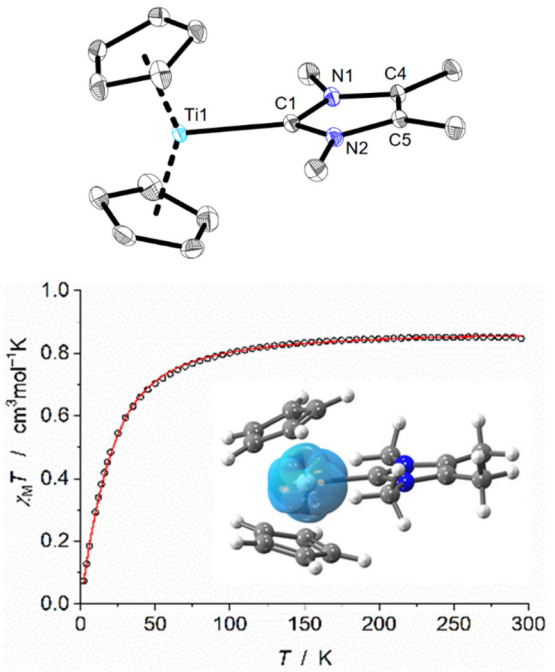

Fig. 2 Top: Molecular structure of [Cp$_2$Ti(IMe$_4$)] (**6**) in the crystal. Anisotropic displacement parameters are drawn at the 50% probability level, with data collected at 100 K (hydrogen atoms omitted for clarity). Selected bond lengths (Å) and angles (deg): Ti1–C1 2.2712(9), C1–N1 1.3624(10), C1–N2 1.3603(10), C4–C5 1.3543(13), Ct1–Ti1–Ct2 144.5, Ct1–Ti1–C1 106.8, Ct2–Ti1–C1 108.6; Bottom: variable-temperature $\chi_M T$ product for **6** (open circles) and best fit curve (red line); Insert: calculated spin density (Triplet; UPBE0-D3BJ/Def2-TZVP; isovalue = 0.15 Å^{-3}).

ESI† for details). The $\chi_M T$ value of 0.85 cm^3 mol^{-1} K at 295 K for **6** clearly indicates $S = 1$ spin state (expected spin-only value of 1.0 cm^3 mol^{-1} K). When the temperature was lowered, the $\chi_M T$ value decreased below ~70 K due to the sizeable zero-field splitting of −43.2 cm^{-1} (Fig. 2, bottom).[19] To evaluate this computationally, the crystallographically derived geometries of **5** and **6** were optimised by density functional theory (DFT) with singlet and triplet wavefunctions, at the (U)PBE0-D3BJ/def2-TZVP level of theory, finding that the triplet states are energetically favoured by ΔE = 9.5 and 13.5 kcal mol^{-1}, respectively.[19] Analysis of the Kohn–Sham molecular orbitals of compound **6** found two occupied quasi-degenerate α-SOMOs with A_1 and B_1 symmetry (assuming a C_{2v} point group), localised at the d_{z^2} and d_{xz} orbitals of the Ti centre. The spin density (Fig. 2, bottom) is also localised around the Ti centre and shows exclusively α-electron density. This is reflected in further analysis by natural bond orbital (NBO) theory, finding two (α) lone particles (two unpaired electrons) at Ti, accounting for 0.91 and 0.84 electrons, respectively. The latter (d_{z^2}) is lower than the former, accounting for delocalisation of electron density onto the metallocene rings, this was located by natural localised molecular orbital (NLMO) theory. Natural population analysis (NPA) gave a low natural charge, and a natural spin close to two (0.63 and 1.79, respectively), also indicative of a Ti(II) triplet system. The spin density on the carbene carbon is negligible. Analysis of dititanium complex **5** by NBO and NPA showed that both titanium centres have comparable NPA charges and are more positive than **6** (0.74, 0.78). Their natural spin densities (0.9, 0.97) place an unpaired electron on each Ti centre, indicating two Ti(III) centres (rather than a mixed valence species). There is no NBO describing a Ti–Ti interaction, thus, each Ti centre can be described as Ti(III) with 17 valence electrons. Inspection of the spin density reveals localisation at the titanium centres, with qualitatively the same d-orbitals which combine on one metal in the case of **6** (d_{z^2} and d_{xz}) (Fig. S30†).

In conclusion, we have synthesised and characterised a series of Zr and Ti metallocenes, produced by the reaction of small NHCs with metallocene sources [Cp_2Zr(py)(btmsa)] (**1**) and [Cp_2Ti(btmsa)] (**2**) which showed varied outcomes. Amongst these, we have developed a highly selective protocol for the synthesis of the parent isolable monomeric triplet Ti(II) metallocene and present our initial analysis of its electronic and magnetic properties. This communication acts as the first step of an in-depth study on Ti(II) triplet organometallics, which will be further explored as novel reagents and molecular spintronic components.

Data availability

The data supporting this article have been included as part of the ESI.† Additional references have been cited within the ESI.†[27–47] Crystallographic data have been deposited at the Cambridge Crystallographic Data Centre (CCDC) under deposition numbers 2419251–2419254 for (**3–6**)† and can be obtained from **https://www.ccdc.cam.ac.uk/structures/**.

Conflicts of interest

There are no conflicts to declare.

Acknowledgements

Financial support (VCI Liebig fellowships for O.P.E.T. and M. F.; YIG Prep Pro fellowship for O.P.E.T.) is gratefully acknowledged. The NMR, MS, and EA services at the Faculty of Chemistry of the Georg-August-Universität Göttingen are kindly acknowledged for measurements and technical assistance. Support from the DFG (INST 186/1237-1 and INST 186/1324-1) is also gratefully acknowledged. The authors acknowledge support by the state of Baden-Württemberg through bwHPC and the German Research Foundation (DFG) through grant no INST 40/575-1 FUGG for access to the JUSTUS 2 cluster.

References

1 Selected recent review articles: (*a*) M. Manßen and L. L. Schafer, *Chem. Soc. Rev.*, 2020, **49**, 6947–6994; (*b*) S. Fortier and A. Gomez-Torres, *Chem. Commun.*, 2021, **57**, 10292–10316; (*c*) U. Rosenthal, *ChemistryOpen*, 2021, **10**, 1234–1243.
2 E. P. Beaumier, A. J. Pearce, X. Y. See and I. A. Tonks, *Nat. Rev. Chem.*, 2019, **3**, 15–34.
3 (*a*) L. C. de Camargo, M. Briganti, F. S. Santana, D. Stinghen, R. R. Ribeiro, G. G. Nunes, J. F. Soares, E. Salvadori, M. Chiesa, S. Benci, R. Torre, L. Sorace, F. Totti and R. Sessoli, *Angew. Chem., Int. Ed.*, 2020, **60**, 2588–2593; (*b*) M. Briganti, G. Serrano, L. Poggini, A. L. Sorrentino, B. Cortigiani, L. C. de Camargo, J. F. Soares, A. Motta, A. Caneschi, M. Mannini, F. Totti and R. Sessoli, *Nano Lett.*, 2022, **22**, 8626–8632; (*c*) S. Wisbeck, A. L. Sorrentino, F. S. Santana, L. C. de Camargo, R. R. Ribeiro, E. Salvadori, M. Chiesa, N. Giaconi, A. Caneschi, M. Mannini, L. Poggini, M. Briganti, G. Serrano, J. F. Soares and R. Sessoli, *Chem. Sci.*, 2024, **15**, 14390–14398.
4 U. Rosenthal, *Chem. Soc. Rev.*, 2020, **49**, 2119–2139.
5 (*a*) M. Polasek and J. Kubista, *J. Organomet. Chem.*, 2007, **692**, 4073–4083; (*b*) P. J. Chirik, *Organometallics*, 2010, **29**, 1500–1517.
6 J. E. Bercaw, *J. Am. Chem. Soc.*, 1974, **96**, 5087–5095.
7 (*a*) P. B. Hitchcock, F. M. Kerton and G. A. Lawless, *J. Am. Chem. Soc.*, 1998, **120**, 10264–10265; (*b*) L. Lukesova, M. Horacek, P. Stepnicka, K. Fejfarova, R. Gyepes, I. Cisarova, J. Kubista and K. Mach, *J. Organomet. Chem.*, 2002, **663**, 134–144; (*c*) L. Lukesova, J. Pinkas, M. Horacek,

R. Gyepes, J. Kubista and K. Mach, *J. Organomet. Chem.*, 2006, **691**, 748–758.
8 (*a*) U. Rosenthal, *Organometallics*, 2020, **39**, 4403–4414; (*b*) U. Rosenthal, *ChemistryOpen*, 2019, **8**, 1036–1047.
9 See for example: (*a*) D. W. Stephan, *Organometallics*, 1992, **11**, 996–999; (*b*) G. Bousrez, I. Dechamps, J.-L. Vasse and F. Jaroschik, *Dalton Trans.*, 2015, **44**, 9359–9362; (*c*) G. Bousrez, D. Harakat, S. Chevreux, I. Déchamps-Olivier and F. Jaroschik, *Dalton Trans.*, 2024, **53**, 15595–15601.
10 (*a*) E. Negishi, F. E. Cederbaum and T. Takahashi, *Tetrahedron Lett.*, 1986, **27**, 2829–2832; (*b*) E. Negishi and S. Huo, in *Titanium and Zirconium in Organic Synthesis*, ed. I. Marek, Wiley-VCH, Weinheim, 2002, pp. 1–49.
11 (*a*) L. B. Kool, M. D. Rausch, H. G. Alt, M. Herberhold, U. Thewalt and B. Wolf, *Angew. Chem., Int. Ed. Engl.*, 1985, **24**, 394–401; (*b*) L. B. Kool, M. D. Rausch, H. G. Alt, M. Herberhold, B. Honold and U. Thewalt, *J. Organomet. Chem.*, 1987, **320**, 37–45.
12 (*a*) J. G. Murray, *J. Am. Chem. Soc.*, 1959, **81**, 752–753; (*b*) J. L. Atwood, K. E. Stone, H. G. Alt, D. C. Hrncir and M. D. Rausch, *J. Organomet. Chem.*, 1975, **96**, C4–C6.
13 (*a*) V. V. Burlakov, A. V. Polyakov, A. I. Yanovsky, Y. T. Struchkov, V. B. Shur, M. E. Vol'pin, Z. Rosenthal and H. Görls, *J. Organomet. Chem.*, 1994, **476**, 197–206; (*b*) U. Rosenthal, A. Ohff, W. Baumann, A. Z. Tillack, H. Görls, V. V. Burlakov and V. B. Shur, *Z. Anorg. Allg. Chem.*, 1995, **621**, 77–83; (*c*) J. R. Nitschke, S. Zürcher and T. D. Tilley, *J. Am. Chem. Soc.*, 2000, **122**, 10345–10352; (*d*) U. Rosenthal, V. V. Burlakov, P. Arndt, W. Baumann and A. Spannenberg, *Organometallics*, 2003, **22**, 884–900; (*e*) M. Fischer, L. Vincent-Heldt, M. Hillje, M. Schmidtmann and R. Beckhaus, *Dalton Trans.*, 2020, **49**, 2068–2072.
14 See for example: (*a*) P. Chirik, *Organometallics*, 2010, **29**, 1500–1517; (*b*) Z. Xi and Z. Li, *Top. Organomet. Chem.*, 2004, **8**, 27–56.
15 J. Klaucke, N. Sinthathurai, C. Golz, O. P. E. Townrow and M. Fischer, *ChemRxiv*, 2024, preprint, DOI:DOI: **10.26434/chemrxiv-2024-4lzc5**.
16 A. W. Addison, T. N. Rao, J. Reedijk, J. van Rijn and G. C. Verschoor, *J. Chem. Soc., Dalton Trans.*, 1984, 1349–1356.
17 R. J. Baker, T. Bannenberg, A. Kunst, S. Randoll and M. Tamm, *Inorg. Chim. Acta*, 2006, **359**, 4797–4801.
18 For a summary of Group 14 NHC complexes and structural parameters see: C. D. Zhang and G. Zi, *Chem. Soc. Rev.*, 2015, **44**, 1898–1921.
19 For details see the ESI.†
20 See for example: (*a*) J. Ruiz and B. F. Perandones, *J. Am. Chem. Soc.*, 2007, **129**, 9298–9299; (*b*) M. Brill, J. Diaz, M. A. Huertos, R. Lopez, J. Perez and L. Riera, *Chem. – Eur. J.*, 2011, **17**, 8584–8595.
21 (*a*) P. Pyykkö and M. Atsumi, *Chem. – Eur. J.*, 2009, **15**, 186–197; (*b*) P. Pyykkö and M. Atsumi, *Chem. – Eur. J.*, 2009, **15**, 12770–12779.
22 N. Tsoureas, J. C. Green and F. G. N. Cloke, *Chem. Commun.*, 2017, **53**, 13117–13120.
23 S. S. Semproni, C. Milsmann and P. J. Chirik, *Organometallics*, 2012, **31**, 3672–3682.
24 (*a*) L. Yang, D. R. Powell and R. P. Houser, *Dalton Trans.*, 2007, 955–964; (*b*) A. Okuniewski, D. Rosiak, J. Chojnacki and B. Becker, *Polyhedron*, 2015, **90**, 47–57.
25 P. Yu, E. F. Murphy, H. W. Roesky, P. Lubini, H.-G. Schmidt and M. Noltemeyer, *Organometallics*, 1997, **16**, 313–316.
26 H. Braunschweig, C. Brückner, M. A. Celik, K. Dück, F. Hupp, T. Kramer, J. Krebs and I. Krummenacher, *Chem. – Eur. J.*, 2015, **21**, 11056–11064.
27 C. Barnett, M. L. Cole and J. B. Harper, *Eur. J. Inorg. Chem.*, 2021, 4954–4958.
28 N. Kuhn and T. Kratz, *Synthesis*, 1993, 561–562.
29 E. Bill, *Simulation of the experimental magnetic data was performed with the julX_2S program*, Max-Planck Institute for Chemical Energy Conversion, Mülheim/Ruhr, Germany.
30 Bruker, *SAINT, V8.40B*, Bruker AXS Inc., Madison, Wisconsin, USA.
31 L. Krause, R. Herbst-Irmer, G. M. Sheldrick and D. Stalke, *J. Appl. Crystallogr.*, 2015, **48**, 3–10.
32 G. M. Sheldrick, *Acta Crystallogr., Sect. A:Found. Adv.*, 2015, **71**, 3–8.
33 G. M. Sheldrick, *Acta Crystallogr., Sect. C:Struct. Chem.*, 2015, **71**, 3–8.
34 O. V. Dolomanov, L. J. Bourhis, R. J. Gildea, J. A. K. Howard and H. Puschmann, *J. Appl. Crystallogr.*, 2009, **42**, 339–341.
35 C. R. Groom, I. J. Bruno, M. P. Lightfoot and S. C. Ward, *Acta Crystallogr.*, 2016, **B72**, 171–179.
36 D. Kratzert, *FinalCif*, *V132*, **https://dkratzert.de/finalcif.html**.
37 M. J. Frisch, G. W. Trucks, H. B. Schlegel, G. E. Scuseria, M. A. Robb, J. R. Cheeseman, G. Scalmani, V. Barone, G. A. Petersson, H. Nakatsuji, X. Li, M. Caricato, A. V. Marenich, J. Bloino, B. G. Janesko, R. Gomperts, B. Mennucci, H. P. Hratchian, J. V. Ortiz, A. F. Izmaylov, J. L. Sonnenberg, D. Williams-Young, F. Ding, F. Lipparini, F. Egidi, J. Goings, B. Peng, A. Petrone, T. Henderson, D. Ranasinghe, V. G. Zakrzewski, J. Gao, N. Rega, G. Zheng, W. Liang, M. Hada, M. Ehara, K. Toyota, R. Fukuda, J. Hasegawa, M. Ishida, T. Nakajima, Y. Honda, O. Kitao, H. Nakai, T. Vreven, K. Throssell, J. A. Montgomery Jr, J. E. Peralta, F. Ogliaro, M. J. Bearpark, J. J. Heyd, E. N. Brothers, K. N. Kudin, V. N. Staroverov, T. A. Keith, R. Kobayashi, J. Normand, K. Raghavachari, A. P. Rendell, J. C. Burant, S. S. Iyengar, J. Tomasi, M. Cossi, J. M. Millam, M. Klene, C. Adamo, R. Cammi, J. W. Ochterski, R. L. Martin, K. Morokuma, O. Farkas, J. B. Foresman and D. J. Fox, *Gaussian 16, Revision A.03*, Gaussian, Inc., Wallingford CT, 2016.
38 A. D. Becke, *Phys. Rev. A:At., Mol., Opt. Phys.*, 1998, **38**, 3098–3100.
39 J. P. Perdew, *Phys. Rev. B:Condens. Matter Mater. Phys*, 1986, **33**, 8822–8824.
40 J. P. Perdew, K. Burke and M. Eznzerhof, *Phys. Rev. Lett.*, 1996, **77**, 3865–3868.

41 C. Adamo and V. Barone, *J. Chem. Phys.*, 1999, **110**, 6158–6170.
42 T. Yanai, D. P. Tew and N. C. Handy, *Chem. Phys. Lett.*, 2004, **393**, 51–57.
43 F. Weigend and R. Ahlrichs, *Phys. Chem. Chem. Phys.*, 2005, **7**, 3297–3305.
44 S. Grimme, J. Antony, S. Ehrlich and H. Krieg, *J. Chem. Phys.*, 2010, **132**, 154104.
45 S. Grimme, S. Ehrlich and L. Goerigk, *J. Comput. Chem.*, 2011, **32**, 1456–1465.
46 *NBO 6.0*, E. D. Glendening, J. K. Badenhoop, A. E. Reed, J. E. Carpenter, J. A. Bohmann, C. M. Morales, C. R. Landis and F. Weinhold, Theoretical Chemistry Institute, University of Wisconsin, Madison, WI, 2013.
47 A. Gilbert, *IQMol 3.1.4*, 2024.